# The $CH_3$ tunnelling sidebands of $\Delta m=0$ studied by dipole-dipole driven low-field NMR in the frequency domain



1989 J. Phys.: Condens. Matter 1 10533

(http://iopscience.iop.org/0953-8984/1/51/023)

J. Phys.: Condens. Matter 1 (1989) 10533–10547. Printed in the UK

# The $CH_3$ tunnelling sidebands of $\Delta m = 0$ studied by dipole–dipole driven low-field NMR in the frequency domain

A J Horsewill and A Aibout
Department of Physics, University of Nottingham, Nottingham NG7 2RD, UK

Received 21 August 1989

**Abstract.** The low-field dipole–dipole driven NMR spectra of materials that contain tunnelling molecular groups have been recorded in the frequency domain. The methyl groups in thioanisole and 2-butanone have tunnelling frequencies of 557 ± 3 kHz and 491 ± 3 kHz respectively. In addition to the sidebands of $\Delta m = \pm 1$ and $\Delta m = \pm 2$, tunnelling sidebands of $\Delta m = 0$ are clearly observed at the tunnel frequency and are reported here for the first time. The intensities of all the sidebands are of similar magnitude. The sidebands of $\Delta m = 0$ result from transitions induced by the RF field in which the methyl group undergoes a change in tunnelling state without a change in overall spin. Despite this, the sidebands are observed in a plot of proton magnetisation versus frequency. A thermodynamic model is proposed to explain how the change in magnetisation is generated; level crossings encountered as part of the field cycling sequence are responsible for transferring disorder in the tunnel reservoir into disorder in the Zeeman reservoir. Discussion also centres upon the mechanism responsible for driving the transitions revealed in the low-field spectra.

## 1. Introduction

In conventional magnetic resonance experiments it can often be advantageous to perform the measurements at high magnetic field. Under these conditions second-order and higher effects in the spectrum resulting from non-secular terms in the Hamiltonian are minimised. Consequently, the interpretation of the spectrum is facilitated since in the high-field regime the observed transitions obey simple selection rules. Furthermore, operation at high magnetic field has considerable advantages in respect of signal to noise ratio. By contrast, in recent years experimental techniques have been developed that exploit certain advantages of performing magnetic resonance in very low or zero magnetic field. One of these is designed to measure the zero-field NMR spectrum in the time domain [1]. Such spectra are very often recorded on powdered samples and the dipolar splittings revealed by the technique can be interpreted to provide crystallographic information in the form of internuclear distances. A second category of experiments, and the subject of this paper, is designed to record low-field proton NMR spectra in the magnetic field or frequency domain [2]. In so doing, non-secular terms in the dipolar Hamiltonian are utilised to drive transitions that are normally considered forbidden in the high-field regime. The resulting spectra can be very rich. A double quantum spectrum is invariably observed with high intensity. In addition sidebands to the main NMR lines

0953-8984/89/5110533 + 15 $02.50  

are present that result from the tunnelling of molecular groups contained in the material. Indeed this spectroscopy has developed as a tool in the investigations of tunnelling phenomena of the methyl molecular rotor, $CH_3$. Tunnelling sidebands have been observed with good intensity in the range 30 kHz $\leq \nu_t \leq$ 1500 kHz.

Investigations of low-field NMR spectra have hitherto been performed in fixed frequency mode. That is to say the spectrum has been recorded as a function of magnetic field and transitions revealed when the NMR transition frequencies match the applied RF frequency of typically 750 kHz. In a new development reported here for the first time we describe a series of investigations in which the NMR spectra have been recorded in the frequency domain. In these experiments the magnetic field has been fixed at zero or very low magnetic field and the frequency swept to record the NMR spectrum. This procedure has the advantage that all transitions are driven under the same conditions of magnetic field.

In this paper we report principally upon the zero-field and very low-field frequency swept NMR spectra of thioanisole. In this material the methyl group is bonded directly to a divalent sulphur atom. In this respect it is similar to the methyl group in dimethyl sulphide in which methyl tunnelling sidebands have previously been observed by low-field NMR [2]. As will become apparent in later discussion, tunnelling sidebands of the $\Delta m = 0$ NMR line have been observed in this investigation. In order to study further the origin of these unexpected components of the low-field spectrum, additional experimental data were recorded upon 2-butanone.

## 2. Experimental details

Low-field NMR spectra have been recorded on thioanisole (methyl-phenyl sulphide $C_6H_5SCH_3$), 2-butanone ($CH_3CH_2COCH_3$) and dimethyl sulphide ($CH_3SCH_3$) at a temperature of 4.2 K. These materials, obtained from the Aldrich Chemical Co., are liquids at room temperature and were encapsulated in small glass capsules under vacuum. In order to obtain good signal to noise ratio in the measured proton magnetisation, all NMR measurements were made at a magnetic field, $B_{spec}$, of either 0.610 T or 0.495 T. The corresponding spectrometer frequencies were 26 MHz and 21.1 MHz respectively. The NMR transitions of interest were driven at low magnetic field by electromagnetic radiation with frequency of order 500 kHz. The high-field measurement and low-field irradiation regimes were bridged by using a rapid field cycling routine as follows:

(a) destroy proton magnetisation at $B_{spec}$ with a train of 90° pulses;

(b) switch field rapidly to 1 T and allow proton magnetisation to grow for time period $t_a$ (typically one minute);

(c) switch rapidly to low magnetic field, $B_r$, and irradiate with electromagnetic radiation of frequency $\nu_{RF}$ for time $t_b$ (typically ten seconds);

(d) switch field rapidly back to $B_{spec}$ and measure proton magnetisation with a single 90° pulse.

This sequence was repeated until a magnetisation destruction spectrum was swept out. Proton magnetisation created during step (b) was destroyed during step (c) when $\nu_{RF}$ matched a transition frequency. There were two modes of operation, either $\nu_{RF}$ was fixed and the field $B_r$ swept, or $B_r$ was fixed and $\nu_{RF}$ swept. Both techniques were employed here. The switching speed of the magnet was approximately 1 T $s^{-1}$ and the characteristic times in the experiment were all much shorter than the spin–lattice

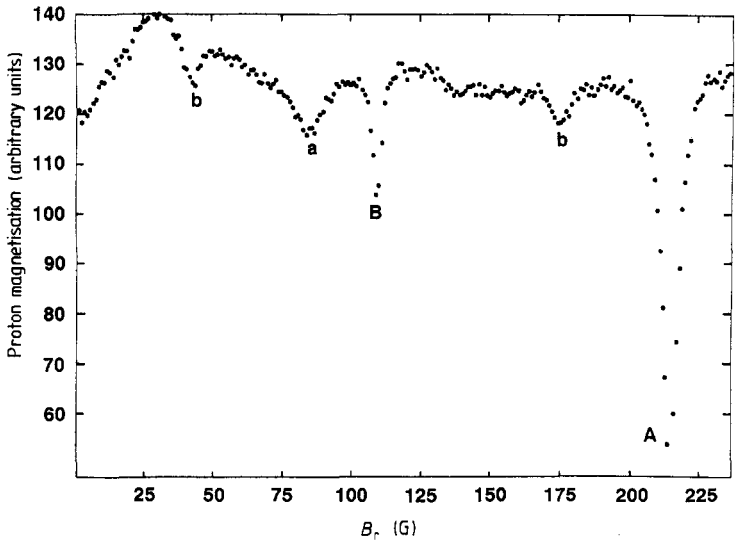


**Figure 1.** The magnetic field swept dipole–dipole driven NMR spectrum of thioanisole recorded at 4 K and with $\nu_{RF}$ = 900 kHz. Letters A and B label the main $\Delta m = \pm 1$ and $\Delta m = \pm 2$ NMR transitions and the letters a and b the corresponding tunnelling sidebands.

relaxation time $T_1$. The latter is long at liquid helium temperatures for the materials studied. It was not necessarily expedient to use samples in which all atmospheric oxygen had been eliminated—otherwise the growth of a measurable quantity of proton magnetisation in step (b) was found to be unacceptably long.

The fast-switching magnet comprised a Nb–Sn superconducting solenoid with inductance 0.2 H. The irradiation at $\nu_{RF}$ was carried out using a pair of broad-band Helmholtz coils placed outside the main NMR coil and orthogonal to it. All operations within the experimental cycle were controlled by microcomputer.

## 3. Results

A magnetic field swept spectrum of thioanisole recorded with $\nu_{RF}$ = 900 kHz is presented in figure 1. The spectrum is presented as a plot of proton magnetisation, $M_Z$, versus magnetic field, $B_r$. The NMR transitions with selection rules $\Delta m = \pm 1$ and $\Delta m = \pm 2$ reveal themselves as holes in $M_Z$ at 211 and 106 G and are labelled A and B respectively. In addition, sidebands to each of these NMR lines are observed and labelled with lower case letters a and b according to whether they belong to A or B. The sidebands result from the tunnelling motion of the methyl group on the molecule of thioanisole. The tunnelling has a single well defined frequency, $\nu_t$, which determines the frequency offset of the sideband from its parent NMR line. Accordingly we deduce the tunnelling frequency for thioanisole to be 557 ± 3 kHz. It is noteworthy that the magnitude of the offset of the tunnelling sidebands of $\Delta m = \pm 1$ is equal to $\nu_t$; by contrast the offset of the $\Delta m = \pm 2$ sidebands is $\nu_t/2$. The scaling factor of two is an artifact of the experimental procedure and arises because the spectrum was recorded in field swept mode. Its value of two

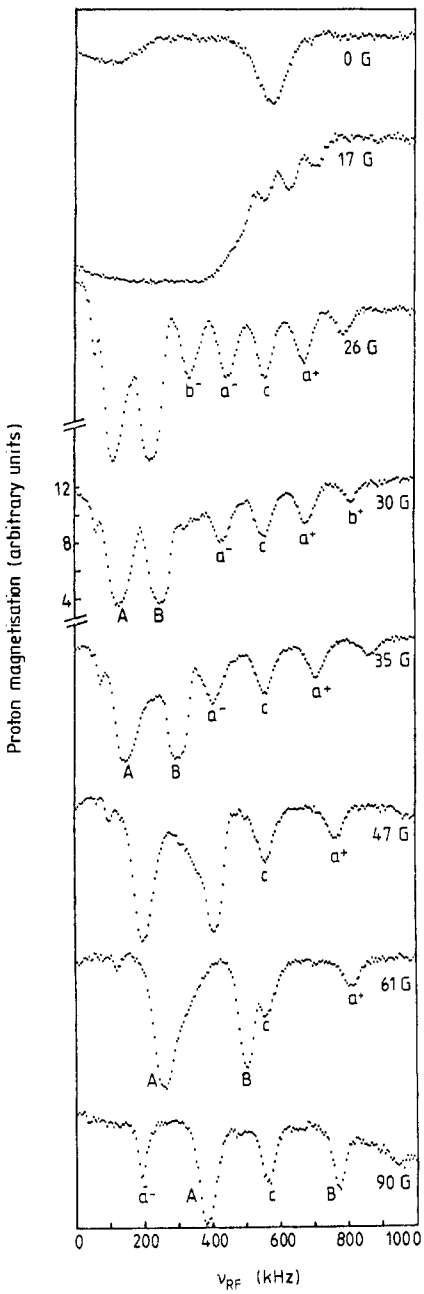


**Figure 2.** The frequency swept dipole–dipole driven NMR spectra of thioanisole recorded at a variety of magnetic fields.

reflects the fact that, during the transition, two nuclei are flipped as one methyl group simultaneously undergoes a change of tunnelling state.

In figure 2 we present the results of experiments designed to record the low-field spectra of thioanisole in the frequency domain. For each spectrum recorded a slightly different fixed magnetic field $B_f$ was chosen in the range 0–90 G. The NMR lines and sidebands are labelled on the diagram according to an extension to the earlier convention

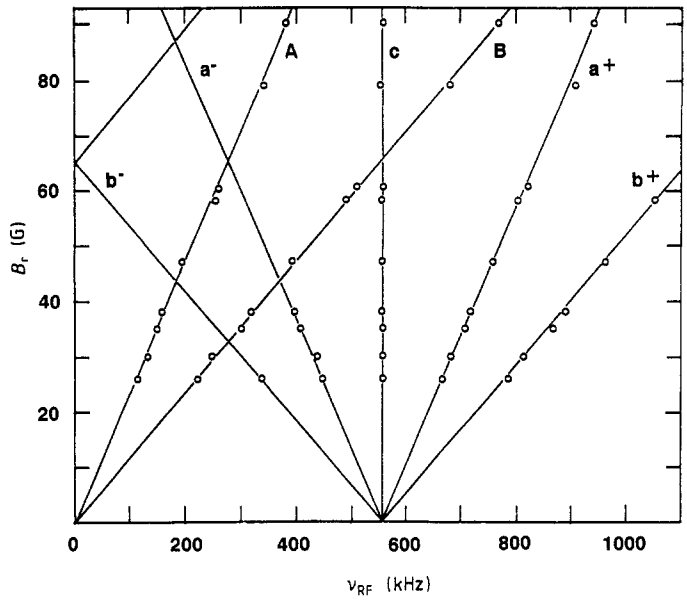


**Figure 3.** The NMR and sideband transitions observed in the thioanisole data of figure 2 presented as a plot of magnetic field versus transition frequency.

in which the + or − superscripts designate the $+\nu_t$ or $-\nu_t$ sidebands. A number of features are noteworthy in these spectra. Firstly, the complication of the scaling factor two for the offsets of the tunnelling sidebands of $\Delta m = \pm 2$ does not arise in frequency swept mode. Sidebands appear at $\pm\nu_t$ on both $\Delta m = \pm 1$ and $\Delta m = \pm 2$ NMR lines. Secondly, the magnetic fields chosen for the scans are sufficiently low that the Larmor frequency $\nu_L$ is less than the tunnel frequency. As a result, the sidebands $(-\nu_t)$ are reflected through the zero-frequency axis and appear at a higher frequency than their parent NMR line.

A third feature is of considerable interest and concerns a new transition which is observed and reported here for the first time. This is a magnetic field independent transition (labelled c in the figures) and it occurs at the tunnelling frequency. It is a transition that involves no overall change in proton spin state yet nevertheless is observed in our plots of proton magnetisation versus frequency. This is a remarkable observation; the RF field has apparently induced a transition without a change in nuclear spin. We shall for convenience describe it as a $\Delta m = 0$ tunnelling peak or sideband and return to discuss its origin in depth in the next section.

The field/frequency dependence of the transitions recorded in figure 2 are summarised in figure 3. As this diagram shows, at finite fields below 20 G there is much overlap between the lines, so the information content of such scans is resolution limited. Finally the relative intensities of the spectral components are worthy of comment. The tunnelling sidebands of $\Delta m = 0$, $\Delta m = \pm 1$ and $\Delta m = \pm 2$ are of similar intensity but they have a tendency to diminish in intensity towards higher frequency. Furthermore, the intensities of these sidebands, which are forbidden in the high-field regime, are a considerable proportion of the intensity of the main $\Delta m = \pm 1$ transition. However, spectra recorded as a function of time, $t_b$, spent at $B_r$ have shown that the $\Delta m = \pm 1$ and

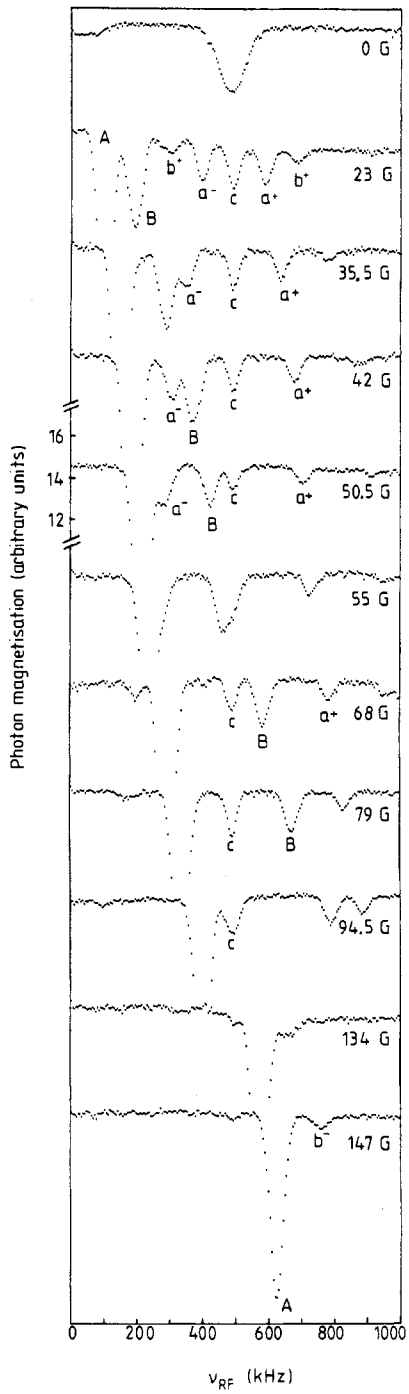


**Figure 4.** The frequency swept dipole–dipole driven NMR spectra of 2-butanone recorded at a variety of magnetic fields.

$\Delta m = \pm 2$ NMR peaks A and B are partially saturated. The finite switching speed of the magnet prevents a quantitative study of this effect at present.

In the zero-field spectrum of figure 2 the $\Delta m = 0$ tunnelling peak occurs with a slight offset from the tunnel frequency at 580 kHz. This offset did not appear to be

systematically dependent upon any experimental variables such as intensity of RF irradiation and no explanation can be offered for its existence at present. A narrow line is also observed in the spectrum at half the NMR frequency. The latter is probably due to low-level harmonics of $\nu_{RF}$ generated by electrical non-linearity in the probe-head.

In order to establish whether the observations above are general to all methyl groups, or whether they are specific to a particular material, we have recorded frequency swept spectra at low field on 2-butanone. Its frequency ($\nu_t = 491 \pm 3$ kHz) has been reported earlier as a result of field swept experiments [3]. (There are two methyl groups in the molecule of 2-butanone; it is the $CH_3$ group on the alkyl chain that is most remote from the carbonyl group that is studied here.) The spectra are presented in figure 4 and are annotated with the convention established earlier. The tunnel frequency is similar to that in thioanisole so the overall features of figures 2 and 4 are similar. The $\Delta m = 0$ peak at the tunnelling frequency is once again present in this material and has a very similar intensity to the $\Delta m = \pm 1$ sidebands; however, the $\Delta m = \pm 2$ sidebands are by comparison both of weaker intensity. A study of figure 4 reveals a pertinent observation when $\nu_L > \nu_t$, since the $\Delta m = 0$ peak then has a considerably diminished intensity and indeed is not visible outside the noise in the background of the scan when $B_r = 147$ G. We shall return to investigate this further in later discussion.

From the evidence supplied by the materials studied here the presence of the $\Delta m = 0$ tunnelling peak at fields where $\nu_L < \nu_t$ does appear to be a general phenomenon. Indeed in figure 5 a zero-field spectrum of dimethyl sulphide is presented and peaks are observed at the known tunnelling frequencies of 95 kHz and 750 kHz.

## 4. Discussion

### 4.1. Background

A methyl group may be idealised as a rigid equilateral triangle of hydrogen atoms. This experiences a three-fold-symmetric potential barrier as a result of the electrostatic interaction with the molecular environment. At low temperature, the dynamics is dominated by quantum tunnelling at a rate which is determined by the magnitude of the barrier. An energy level diagram that summarises many of the salient features of the NMR spectroscopy of methyl tunnelling is presented in figure 6. This has been calculated by diagonalisation of the Hamiltonian matrix in the simple basis $|m_I^1 m_I^2 m_I^3\rangle$, where the time independent Hamiltonian is given by

$$H = H_Z + H_d + H_t. \tag{1}$$

Here $H_Z$ is the Zeeman Hamiltonian for the three proton spins,

$$H_Z = -\hbar\gamma \sum_{j=1}^{3} B_Z I_{jZ}. \tag{2}$$

$H_d$ represents the dipole–dipole interaction between the protons on the methyl group and is expressed following the notation of Wolf [4] as a scalar product of two second-rank tensors representing spin and spatial contributions. The suffices $j$ and $k$ label the protons,

$$H_d = \sum_{j>k}^{3} \sum_{q=0}^{2} A_{jk}^{(q)} \cdot F_{jk}^{(q)}. \tag{3}$$

In performing the numerical calculations the full untruncated form of $H_d$ was employed;

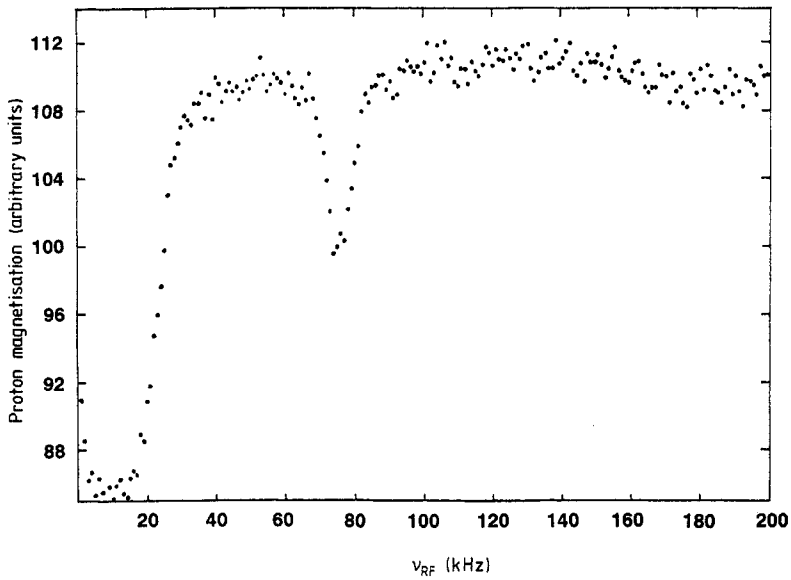


**Figure 5.** The dipole–dipole driven NMR spectrum of dimethyl sulphide recorded at zero field

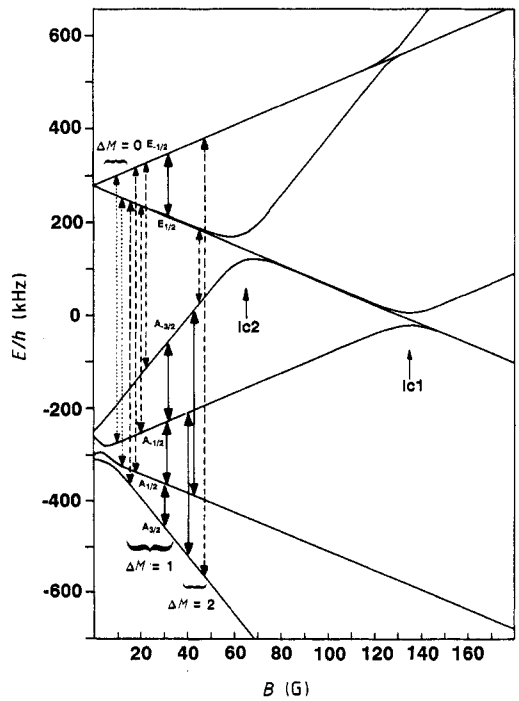


**Figure 6.** The energy level diagram of a tunnelling methyl group ($\nu_t$ = 557 kHz) recorded as a function of magnetic field.

furthermore, the spatial part $F_{jk}^{(g)}$ was calculated assuming tetrahedral symmetry and C–H bonds-lengths of 1.0 Å. $H_t$ describes the exchange resulting from the tunnelling dynamics. The associated energy shifts, $h\nu_t = 3J$, have been incorporated with the use of an equivalent spin operator [5].

$$H_t = -2J \sum_{j>k}^{3} I_j \cdot I_k. \tag{4}$$

In figure 6 the enegy levels have been calculated as a function of the magnitude of the magnetic field applied in an arbitrary but known direction. At zero field there are two fourfold degenerate states labelled A and E according to the irreducible representations of the group $C_3$. The A state is the ground state and is a nuclear spin $\frac{3}{2}$. The E state is a doublet (sub-levels labelled $E^a$ and $E^b$) of nuclear spin doublets of spin $\frac{1}{2}$. The degeneracies may be lifted at zero field by the dipole–dipole interaction. Symmetry arguments applicable in the low-temperature, pure quantum tunnellling regime demand that the spin and spatial degrees of freedom are coupled together (see [5], [6]). The physically feasible permutations of the protons within a methyl group correspond to rotations of the whole group by 120° and this involves a double exchange of protons. Consequently the Pauli principle requires that the total wavefunction must be symmetrical with respect to 120° rotation. The acceptable space–spin product wavefunctions are therefore restricted to the following combinations; $A \times A$, $E^a \times E^b$ and $E^b \times E^a$. This is the origin of the coupling between space and spin degrees of freedom, and the tunnelling states are properly described as spin-symmetry species. We shall label the product wavefunctions according to a convention of which the following is an example; $E^a \cdot E^b_{1/2}$. Here the first term represents the spatial part and the second the spin, the latter incorporating a subscript to designate the spin state. The spin wavefunctions are given as follows [7]:

$$A_{3/2} = |\alpha\alpha\beta\rangle$$

$$A_{1/2} = (1/\sqrt{3})(|\alpha\alpha\beta\rangle + |\alpha\beta\alpha\rangle + |\beta\alpha\alpha\rangle)$$

$$E^a_{1/2} = (1/\sqrt{3})(|\alpha\alpha\beta\rangle + \varepsilon|\alpha\beta\alpha\rangle + \varepsilon^*|\beta\alpha\alpha\rangle)$$

$$E^b_{1/2} = (1/\sqrt{3})(|\alpha\alpha\beta\rangle + \varepsilon^*|\alpha\beta\alpha\rangle + \varepsilon|\beta\alpha\alpha\rangle).$$

The wavefunctions for negative $m_I$ may be obtained by interchanging $\alpha$ and $\beta$. In order to observe a transition involving a change in tunnelling state, the Hamiltonian mediating the transition must couple spatial and spin degrees of freedom and have the appropriate symmetry. This requirement is met by the dipole–dipole interaction.

The transition frequencies in the low-field NMR spectra are determined by splittings between states in the energy level diagram of figure 6. Pure NMR transitions $\Delta m = \pm 1$ and $\Delta m = \pm 2$ are labelled by full lines and involve a change of spin state only. Transitions may also take place in which a change in tunnelling state occurs simultaneously with a change in spin state; these give rise to the sidebands in a low-field spectrum and are represented by broken lines in figure 6. Of all these transitions, only the $\Delta m = \pm 1$ is not forbidden at high magnetic field. It is only at low magnetic field—where the proton Zeeman splittings are of the order of the dipolar energies—that the $\Delta m = \pm 2$ and sideband transitions become allowed. Further discussion of the transition mechanism will be deferred to section 4.3.

*4.2. The $\Delta m = 0$ tunnelling peak*

The observation of the magnetic field independent $\Delta m = 0$ tunnelling transition in the low-field spectrum is a remarkable one. This corresponds to a transition that involves a change in tunnelling state but with no overall change in proton spin state. For this reason it is paradoxical that the transition should be observed at all in an experiment designed to measure changes in proton magnetisation. We propose that the answer lies in the nature of the field cycling technique employed to study the low-field NMR spectrum.

The model that is proposed to explain the $\Delta m = 0$ peak is a thermodynamic one. According to accepted practice we may assume that the tunnelling energy resides in a thermal reservoir, with an inverse temperature $\beta_t$, which is only weakly coupled to the lattice. The proton Zeeman energy also has its own thermal reservoir with inverse temperature $\beta_Z$; again this only weakly coupled to the lattice, particularly at low temperature where $T_1$ is long. Under normal conditions the tunnelling and Zeeman reservoirs are isolated from each other. A more detailed discussion of the mechanism by which transitions are induced at low field by the RF irradiation will be given in section 4.3. For the purposes of discussion here we assume that the RF field is able to drive A–E tunnelling transitions within the tunnelling reservoir without an overall change in proton spin. This results in a change in the tunnelling temperature. Under normal circumstances this change does not communicate itself to the Zeeman reservoir; however, it has been shown in tunnel resonance spectroscopy [8] that at the level-crossings indicated on figure 6 the energy is free to move between the tunnelling and Zeeman reservoirs. The level-crossings occur when $\nu_t = \nu_L$ (lc1) and $\nu_t = 2\nu_L$ (lc2). In this way the RF induced heating that has taken place in the tunnelling reservoir is communicated to the Zeeman reservoir as the level-crossings are encountered during the period when the field is switched rapidly from $B_r$ to $B_{spec}$. This can lead to a measurable change in the proton magnetisation.

The behaviour has been modelled with the aid of a computer; the thermodynamics of the field switches and the level-crossings follow the model used by Clough *et al* [9] in their successful description of the tunnel resonance spectrum of acetone. The salient features of the model are as follows. Prior to the low-field scan the tunnel reservoir was assumed to have a temperature $1/\beta_t = 10$ K. As will become apparent this value is modified as each measurement in the cycle is performed and $\beta_t$ moves towards a quasi-equilibrium value. The first procedure in each cycle of the low-field experiment is to saturate $M_Z$ and subsequently allow a known magnetisation to grow. In the thermodynamic model this corresponds to establishing a known finite temperature in the Zeeman reservoir; in our numerical simulation $1/\beta_Z$ was taken to be 100 K before each individual measurement in the scan. When the field is switched between magnetic fields $B_1$ and $B_2$, without passing through a level-crossing, then we make an adiabatic assumption and preserve the magnetisation. Consequently $\beta_Z$ changes to $(B_1/B_2)\beta_Z$. When a level crossing is encountered then the Zeeman and tunnel temperatures instantaneously thermalise and a common temperature, $(C_Z\beta_Z + C_t\beta_t)/(C_Z + C_t)$, is established in the two reservoirs. Here the heat capacities of the two reservoirs $C_Z$ and $C_t$ are given by the spacings between the eight energy levels of the $CH_3$ group,

$$C_Z \propto h\nu_L[2 \times (\tfrac{3}{2})^2 + 6 \times (\tfrac{1}{2})^2] \qquad C_t \propto h\nu_t[8 \times (\tfrac{1}{2})^2].$$

Hence at the level-crossing where $\nu_L = \nu_t$ then $C_t/C_Z = \frac{1}{3}$ and at the level-crossing where $2\nu_L = \nu_t$ then $C_t/C_Z = \frac{4}{3}$. One final detail concerns the heating of the tunnel reservoir by the RF field at the tunnel frequency. If $Q$ is proportional to the transition probability,

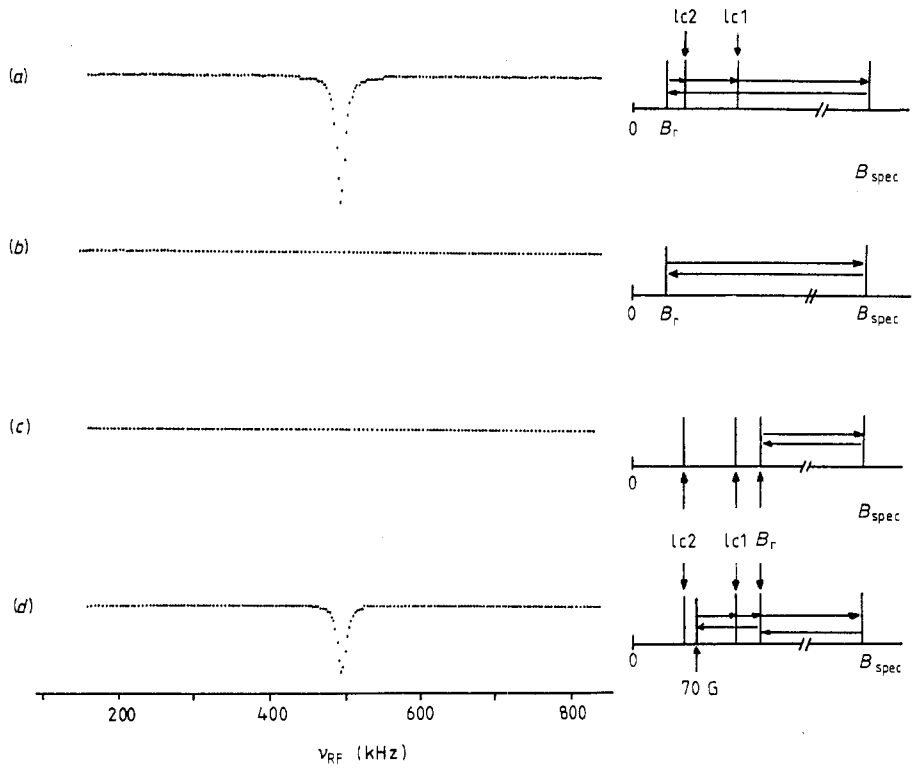


**Figure 7.** Computer simulations of the thermodynamic model depicting the $\Delta m = 0$ tunnelling sideband. The insets, plotted as a function of magnetic field, describe the sequence of field switches and level-crossings encountered in the experiment. (lc1 and lc2 designate the two level-crossings). (*a*) Low-field NMR spectrum for $\nu_L < \nu_t$. (*b*)As for (*a*) but without equilibration at the level-crossings. (*c*) Low-field NMR spectrum for $\nu_L > \nu_t$. (*d*) As for (*c*) but with a sequence tailored to encounter a level-crossing.

then upon irradiation the inverse tunnel temperature, $\beta_t$, is modified to become $\beta_t/(1 + Q)$. $Q$ was assumed to be a Lorentzian centred at $\nu_t$.

The results of the simulations are shown in figure 7. In figure 7(*a*) $B_r$ was chosen such that $\nu_L < \nu_t/2$ and each step in the simulation is labelled on the inset stick diagram. Following irradiation at $B_r$ the magnetic field is switched back to $B_{spec}$ passing through the level-crossings and equilibrating the Zeeman and tunnel temperatures as it goes. It is in this final stage that the disorder in the tunnel reservoir is transformed to disorder in the Zeeman reservoir with a corresponding change in the proton magnetisation. An inverted peak is clearly seen in the spectrum in agreement with experiment. In figure 7(*b*) an identical scan was performed but the equilibration of the reservoir temperatures at the level-crossings was omitted; no feature is observed at the tunnel frequency. A similar null result is obtained if the RF irradiation is omitted from the simulation.

In figure 7(*c*) $B_r$ was chosen such that $\nu_L > \nu_t$, under these circumstances no level-crossings are encountered as the field is switched back to $B_{spec}$. Again in agreement with experiment no features are observed at $\nu_t$. In order to observe a $\Delta m = 0$ peak, the crucial step is clearly the thermalisation of the reservoirs at the level-crossings. The simulation in figure 7(*c*) has been repeated in figure 7(*d*) except that an extra field switch

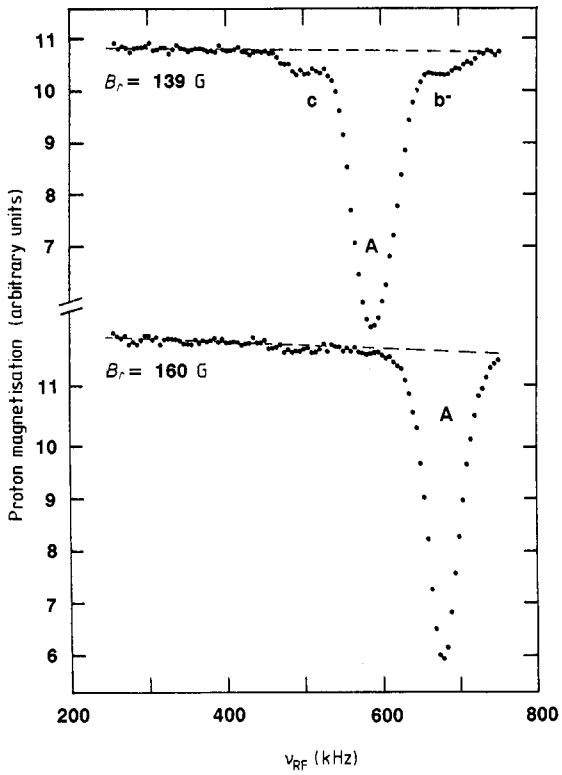


**Figure 8.** Experimental data on 2-butanone for $\nu_L > \nu_t$ using the modified field scan of figure 7(*d*).

been incorporated down to 70 G following RF irradiation and prior to measurement of $M_Z$ at $B_{spec}$. In this way a level-crossing is encountered by design in the experiment. A $\Delta m = 0$ peak is indeed observed in the simulation; its intensity, however, is only half of the intensity of the peak generated by the simulation in figure 7(*a*). This modification to the experiment has been performed on the sample of 2-butanone and the results are presented in figure 8. Measurements have been made for $B_r = 139$ G and $B_r = 160$ G. In the former, a weak $\Delta m = 0$ peak is observed. In the latter, there is no evidence of a $\Delta m = 0$ peak. The idealised thermodynamic model has apparently failed in its application to the high-field data. However one implicit assumption made in the model is open to question, namely that of a field independent transition probability $Q$. As the high-field regime is approached this will inevitably become smaller. It is well established experimentally that the subject of the transition probabilities for dipole–dipole driven NMR is one of some complexity. For example in many studies the $a^-$ sideband is missing entirely whereas the $a^+$ sideband appears with good intensity [2]. Indeed this is also true of the spectra presented here for the higher values of magnetic field. In another investigation on acetophenone [10] it was shown experimentally how the sideband transition probability became enhanced close to the level-crossing lc2. Further discussion is made in section 5 following an account of the matrix elements responsible for driving the sideband transitions.

### *4.3. The dipole–dipole driven nature of the low-field transitions*

We now centre our discussion upon the mechanism whereby transitions are induced between the energy levels in figure 6 to produce the low-field NMR spectra. The interaction of the RF field with the nuclei has A symmetry and so cannot directly drive transitions that involve a change in the tunnelling state. The clear existence of the $\Delta m = 0$ tunnelling peak and the sidebands of $\Delta m = \pm 1$ and $\Delta m = \pm 2$ with similar intensities suggests that a more complicated mechanism is responsible and that it has a similar origin for all tunnelling sidebands. Furthermore because the Zeeman splitting is of similar magnitude to the dipolar energies, the tunnelling splitting and (in appropriate units) the magnitude of the applied RF field, time dependent perturbation theory is not applicable. As described by Clough *et al* [2] in their original paper upon the application of low-field NMR to the study of molecular tunnelling, the answer lies in the dipole–dipole interaction. This has terms connecting spatial and spin degrees of freedom and also spin operators capable of driving one or two simultaneous spin flips. By performing a transformation of the time dependent Hamiltonian into the doubly rotating frame, the time dependence of the RF field may be incorporated into the static Zeeman Hamiltonian. Here it is envisaged that the $z$-direction coincides with the instantaneous resultant field, the latter being a vector sum of applied static and RF fields. In performing this transformation part of the dipole–dipole interaction becomes time dependent and may be employed by the system to drive transitions. In this scheme the $\Delta m = \pm 1$ and $\Delta m = \pm 2$ NMR transitions would be of similar intensity as is indeed the case experimentally. We view the transitions as being driven by the dipole–dipole interaction modulated by the applied RF field.

The dipolar Hamiltonian may be written in symmetry adapted form as follows:

$$H_d = H_d^A + H_d^{E^a} + H_d^{E^b}$$

where

$$H_d^A = \tfrac{1}{3}(A_{12}^{(q)} + A_{23}^{(q)} + A_{31}^{(q)})(F_{12}^{(q)} + F_{23}^{(q)} + F_{31}^{(q)})$$

$$H_d^{E^a} = \tfrac{1}{3}(A_{12}^{(q)} + \varepsilon A_{23}^{(q)} + \varepsilon^* A_{31}^{(q)})(F_{12}^{(q)} + \varepsilon^* F_{23}^{(q)} + \varepsilon F_{31}^{(q)})$$

$$H_d^{E^b} = \tfrac{1}{3}(A_{12}^{(q)} + \varepsilon^* A_{23}^{(q)} + \varepsilon A_{31}^{(q)})(F_{12}^{(q)} + \varepsilon F_{23}^{(q)} + \varepsilon^* F_{31}^{(q)}).$$

Here $\varepsilon = \exp(2\pi i/3)$ and the superscripts on $H_d$ label the symmetry of the spin dependent part. In evaluating the matrix elements of $H_d$ the spatial and spin degrees of freedom are separable, so the corresponding elements may be calculated separately. Furthermore, symmetry arguments may be employed to identify those matrix elements that are non-zero since in such cases the direct product of the symmetry species involved in the bracket and operator must be of A symmetry. Now consider the terms in $H_d$ in which $q = 0$; these contain spin operators like $I_{j+} I_{k-}$ and matrix elements such as

$$\langle A . A_{1/2} | (I_{1+} I_{2-} + \varepsilon I_{2+} I_{3-} + \varepsilon^* I_{3+} I_{1-})(F_{12}^{(0)} + \varepsilon^* F_{23}^{(0)} + \varepsilon F_{31}^{(0)}) | E^a . E_{1/2}^b \rangle$$

are finite. Consequently when the time dependence is incorporated into $H_d$ in the manner described above, then this matrix element is able to drive the transition $A . A_{1/2} \rightarrow E^a . E_{1/2}^b$. The result is a change of tunnelling state without a change of overall spin. Such a transition is labelled as a broken line in figure 6 and gives rise ultimately to a $\Delta m = 0$ tunnelling peak. The mechanism is similar to the one that occurs in spin diffusion, the difference being that there is a frequency offset here which is equal to $\nu_t$, the energy for which is supplied by the RF field. Note that in transforming to the

rotating frame the spin quantisation axes are modified; this has no material effect on the arguments presented here.

We may also select terms for example in $q = 1$; this contains spin operators like $I_{jZ}I_{k+}$, so matrix elements such as

$$\langle A.A_{3/2}|(I_{1Z}I_{2+} + \varepsilon I_{2Z}I_{3+} + \varepsilon^* I_{3Z}I_{1+})(F_{12}^{(1)} + \varepsilon^* F_{23}^{(1)} + \varepsilon F_{31}^{(1)})|E^a.E_{1/2}^b\rangle$$

are available to drive the tunnelling sidebands of $\Delta m = \pm 1$. In a similar way the sidebands $\Delta m = \pm 2$ may be driven by spin operators corresponding to $q = 2$. For example $I_{j-}I_{k-}$ is available for driving the transition $A.A_{3/2} \rightarrow E^b.E_{-1/2}^a$. Since the magnitudes of these matrix elements are all similar, the intensities of the $\Delta m = 0$, $\Delta m = \pm 1$ and $\Delta m = \pm 2$ sidebands are all of similar magnitude in agreement with experiment.

The discussion above has considered only intra-molecular contributions to $H_d$ confined within a particular methyl group. Inter-molecular contributions relating to dipole–dipole interactions between methyl protons and other protons in the lattice are also available to drive the transitions.

## 5. Summary and concluding remarks

We have reported upon a series of investigations in which low-field NMR spectra have been recorded in the frequency domain of materials that contain tunnelling methyl groups. The tunnelling frequencies have been measured but the most significant observation is that of a $\Delta m = 0$ peak which occurs at the tunnelling frequency. The transition itself involves no overall change in proton spin state but matrix elements are available to enable the RF field, in collaboration with the dipole–dipole interaction, to drive A–E tunnelling transitions. This results in an increase in the temperature of the tunnelling reservoir. It has been proposed that the observed changes in the proton magnetisation are generated as a result of the thermalisation of the Zeeman and tunnelling reservoirs at level-crossings which are encountered as part of the field cycling procedure. The idealised thermodynamic model presented to explain this mechanism is shown to have limitations above 100 G but these are probably due to an incomplete description of the magnetic field dependence of the transition probabilities. It has been well known for example since the earliest work in this field [2] that certain transitions can be completely absent from the spectrum and that peak intensities can vary in an as yet unpredictable way. However, the discovery of the $\Delta m = 0$ peak and the role of the level-crossings in the experiment has been given a new perspective to theoretical efforts to achieve a comprehensive and accurate description of these low-field spectra. For example it is clear that the mechanism by which magnetisation changes take place at level-crossings will not be limited to the $\Delta m = 0$ tunnelling peak. Similar changes must also arise from the main NMR and sideband transitions. The extent to which these affect the spectrum is under investigation. Furthermore the fact that the RF field is able to drive A–E tunnelling transitions in the absence of an overall change of spin provides more scope in future experiments for preparing the tunnel reservoir in a predetermined state prior to experimental studies.

## Acknowledgments

This work was funded by a grant from the Science and Engineering Research Council. The authors wish to express their thanks to Professor S Clough for helpful comments

and discussions in connection with this work. AA gratefully acknowledges the award of a postgraduate scholarship from the Ministry of Higher Education, Algeria.

## References

[1] Weitekamp D P, Bielecki A, Zax D, Zilm K and Pines A 1983 *Phys. Rev. Lett.* **50** 1807
[2] Clough S, Horsewill A J, McDonald P J and Zelaya F O 1985 *Phys. Rev. Lett.* **55** 1794
[3] Abed K J, Clough S, Horsewill A J and Mohammed M A 1988 *Chem. Phys. Lett.* **147** 624
[4] Wolf D 1979 *Spin Temperature and Nuclear Spin Relaxation in Matter* (Oxford: Clarendon)
[5] Apaydin F and Clough S 1968 *J. Phys. C: Solid State Phys.* **1** 932
[6] Freed J H 1965 *J. Chem. Phys.* **43** 1710
[7] Haupt J 1971 *Z. Naturf.* a **26** 1578
[8] Clough S and Horsewill A J 1982 *Phys. Rev.* B **25** 4911
[9] Clough S, Horsewill A J and McDonald P J 1984 *J. Phys. C: Solid State Phys.* **17** 1115
[10] Alsanoosi A M, Horsewill A J and Clough S 1989 *J. Phys. C: Solid State Phys.* **1** 643